Engineering Flowfields and Heating Rates for Highly Swept Wing Leading Edges

John J. Bertin,* Stewart J. Mosso,† Daniel W. Barnette,†
University of Texas, Austin, Texas

and

Winston D. Goodrich‡
NASA Johnson Space Center, Houston, Texas

An engineering flow model has been developed and verified experimentally, describing the flowfield which results when a supersonic stream encounters a wedge:cylinder configuration whose angles are such that the flow includes only weak shock waves. A numerical code using the perfect gas relations has been developed to describe the flow in the plane of symmetry inboard of the shock interaction region. Theoretical surface-pressure and heat-transfer distributions were computed for freestream velocities from 1167 m/sec to 7610 m/sec. Nondimensionalization of the heat-transfer rates in terms of local flow parameters produced a correlation, i.e., Stanton number as a function of the local Reynolds number, which was independent of the freestream flow conditions and of the surface temperature.

Nomenclature

C_p = pressure coefficient
h = metric coefficient, Eq. (4), or the local heat-transfer coefficient $\dot{q}/(T_r - T_w)$
h_r = recovery enthalpy
$h_{t,\text{ref}}$ = reference heat-transfer coefficient, $\dot{q}_{t,\text{ref}}/(T_t - T_w)$
h_w = wall enthalpy
M_∞ = freestream Mach number
p = static pressure
$\dot{q}$ = local heat-transfer rate
$\dot{q}_{t,\text{ref}}$ = heat-transfer rate at the stagnation point of a reference sphere
r = radial distance from the axis of the cylinder
r_{le} = radius of curvature of the cylindrical leading-ege
r_s = radius of curvature for a particular streamline
Re_x = Reynolds number, Eq. (6)
St = Stanton number, Eq. (5)
T_r = recovery temperature
T_t = stagnation temperature
T_w = wall temperature
u = streamwise velocity component
U_∞ = freestream velocity
$U_{c.o}$ = circular orbit velocity (7907 m/sec)
x,y,z = leading-edge fixed coordinate system (Fig. 2)
δ = turning angle of wedge element (Fig. 1)
Λ = sweep angle (Fig. 1)
Λ_s = deflection angle for cylindrical element (Fig. 1)
μ_e = viscosity at the edge of the boundary layer
ρ = density

Received Feb. 6, 1976; revision received April 22, 1976. This work was supported by the Johnson Space Center, NASA, Contract NAS9-13680.

Index categories: Boundary Layers and Convective Heat Transfer – Laminar; Jets, Wakes, and Viscid-Inviscid Flow Interactions.

*Associate Professor, Department of Aerospace Engineering and Engineering Mechanics. Member AIAA.

†Research Assistant, Department of Aerospace Engineering and Engineering Mechanics.

‡Research Engineer, Structures and Mechanics Division. Member AIAA.

Introduction

CALCULATIONS based on engineering models of the Shuttle Orbiter entry flowfield, coupled with heat transfer and pressure data from wind tunnel tests, are currently being used to establish methodologies to support vehicle design and trajectory shaping studies. Specifically, the flowfield perturbation which results when the fuselage-generated shock wave interacts with the wing-generated shock wave is particularly important in the design of the Orbiter wing leading-edge. Because of the complexity of the viscid-inviscid interaction phenomena, many experimental investigations of the locally perturbed flowfields use models consisting of elementary configurations, such as wedge: cylinder configurations. As the angle between the wedge surface and the cylinder axis decreases, a distinct change occurs in the structure of the flowfield created by the intersecting waves. The investigations of Hiers and Loubsky,[1] which considered cylinder sweep-angles of 0°, 22.5°, and 45°, of Beckwith[2] (cylinder sweep-angles of 20°and 60°); and of Bushnell[3] (cylinder sweep-angles of 45°and 60°) provided valuable information about shock-interaction patterns. However, it was not until the systematic investigations of Edney,[4] that detailed flow models of the various shock-interaction patterns could be established as a function of sweep angle.

Hains and Keyes[5] have categorized the shock-interaction patterns obtained for a variety of Shuttle configurations in terms of the flow models of Edney. Bertin et al.[6] examined surface-pressure and heat-transfer-rate data for a variety of Shuttle Orbiter configurations over an angle-of-attack range from 0°-60°. The correlations for these three-dimensional flows indicated that the type of shock-interaction pattern was dominated by the effective sweep angle of the leading edge. For the relatively low sweep angles of the straight-wing Orbiters, the interaction between the bow-generated shock and the wing-generated shock wave exhibited the characteristics of a Type V shock-interaction pattern. For delta-wing Orbiters, the shock:shock interaction exhibited the characteristics of a Type VI pattern for all angles of attack. The data discussed above were obtained in facilities where real gas effects would not be expected to significantly alter the shock-interaction phenomena. By comparing data from facilities using helium, air, nitrogen, and tetrafluoromethane as test gases, Hunt and Creel[7] studied the effect of the shock-density ratio on the

body-shock:wing-shock interaction. The effect of the shock-density ratio, or equivalently the specific heat ratio (gamma), was found to be more significant to the Type V pattern than to the Type VI pattern.

Two numerical codes were developed to study what effect the thermodynamic properties of air had on the two-dimensional flowfield which results when supersonic flow encounters double-wedge configurations. One code used the perfect-gas relations, while the second incorporated a Mollier table to define the equilibrium properties for air. Using the numerical codes described in Ref. 8, both the Type V and the Type VI shock-interaction patterns were found to exist theoretically for a given geometry subject to a given flow condition. Thus, an experimental investigation os supersonic flow past double-wedge configurations was conducted in the University of Texas Supersonic Wind Tunnel. Over the range of geometries tested, it was found that, whereas theoretical solutions both for a Type V pattern and for a Type VI pattern could be generated for a particular flow condition (as defined by the geometry and the freestream conditions), the weaker, Type VI pattern was observed experimentally.[9]

Theoretical solutions generated using the numerical code for the Type VI flow pattern were used to study the effects of the freestream conditions and of the real-gas properties on the character of the interactions and on the surface pressures and heating rates. Using the appropriate properties for equilibrium air, i.e., the real-gas solutions, the minimum sweep angle for which a Type VI pattern existed decreased as the freestream velocity increased. The theroetical values for the local heat-transfer rate were divided by the heat-transfer rate at the stagnation point of a reference sphere at the same freestream conditions. Both for the perfect-gas solutions and the real-gas solutions, the nondimensionalized heat-transfer rate was found to increase significantly with velocity inboard of the interaction region. The dimensionless heating for the reentry velocity was roughly twice that for a wind-tunnel condition.

The present investigation was undertaken in order to determine the effect of cross flow, i.e., three-dimensionality, on the wing-leading-edge flow. A wedge:cylinder configuration exposed to a supersonic stream was used to simulate the interaction between the fuselage-generated shock wave and the wing-generated shock wave for both the theoretical and the experimental phases of the effort. The Type VI shock-interaction pattern is modeled, since the previous investigations indicate that it is the more relevant for the Orbiter wing-leading-edge. Since similar velocity-dependent increases in the heat-transfer-rate ratio occurred both for the perfect-gas solutions and for the real-gas solutions, the present investigation considered only the perfect-gas relations for air. Furthermore, the present code only provides solutions for the plane of symmetry in the region inboard of the interaction where the velocity-dependent increase in the nondimensionalized heat-transfer had been found to be the greatest for the two-dimensional configuration. The present effort includes the development of a numerical code to generate perfect-gas solutions for the flowfield in the plane of symmetry along the wing leading edge, the experimental verification of the flowfield model used in the code, and the use of the code to generate the inviscid flowfield and a laminar boundary-layer solution for freestream velocities for 1167 m/sec (3829 fps) to 7610 m/sec (25,000 fps). The present paper discusses the results of this experimental and theoretical investigation.

Theoretical Analysis

As has been discussed, the shock interaction for the delta-wing Orbiter exhibits the characteristics of a Type VI pattern. As indicated in the sketch of Fig. 1, the Type VI interaction includes: 1) the undisturbed freestream flow; 2) the flow turned through the angle δ by a single wave; 3) the flow along the wing-root leading edge which has passed through two

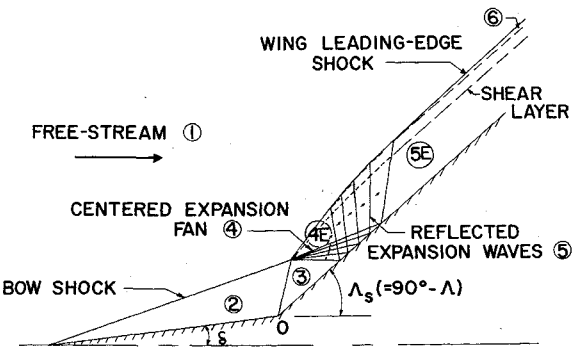

Fig. 1 Flow model for the Type VI shock-interaction pattern.

shock waves; 4) the flow processed by the right-running waves of the expansion fan; 5) the flow which passes through the left running waves produced by the reflection of the waves of the expansion fan; and 6) the flow turned by the wing leading edge through a single shock wave. The flow in region 3 has passed through two shock waves, while the flow in region 6 (which is further outboard) has passed through a single, weak shock and is, therefore, at a lower pressure than that in region 3. Thus, the flow undergoes an expansion, i.e., an acceleration, from the root region to equalize pressure.

A sketch of the theoretical model for the flowfield in the wing-root region is presented in Fig. 2. The simulated bow shock wave was generated when the supersonic freestream encountered the wedge. Thus, for the present investigation, the flow in region 2 was two-dimensional and uniform. The cylinder, i.e., the simulated wing leading edge, was inclined relative to the wedge such that the flow downstream of the wing-root shock wave remained supersonic. (Since only region 3 was considered in the present investigation, the results would be applicable to the Type V interaction as well as the Type VI interaction). The three-dimensional character of the flow in the shock layer caused the wing-root shock wave to be curved. The x-y plane of Fig. 2 is the plane of symmetry for the swept cylinder. The streamtube method was used in the present study to calculate the effect of cross-flow on the shock structure and on the fluid properties in this region.

The sketch of the streamtube pattern which was used to calculate the inviscid flow in the plane of symmetry for region 3 is presented in Fig. 3. The procedure began with the element at the root of the swept cylinder, i.e., element (1,1), and proceeded downstream. Since the flow conditions in region 2 and the turning angle ($\Lambda_s - \delta$) were defined at this point, the initial calculation of the downstream flow properties was made while assuming the two-dimensional (wedge) value for the shock-wave angle. With these values for the flow properties of element (1,1), the cross-flow velocity for the fluid leaving the element (see Fig. 2) was calculated using the linear approximation

$$w = (dw/dz)\ \Delta z \tag{1}$$

The required transverse velocity gradient was determined by using the stagnation region correlation for modified Newtonian flow.

$$dw/dz = (1/r)\,[2p/\rho]^{1/2} \tag{2}$$

No subscripts appear in Eqs. (1) and (2), since they were used not only for (1,1) but for every element. The flow properties and the radial distance from the axis of the cylinder were evaluated for the particular element in the shock layer where the cross-flow was to be evaluated. The shock-wave angle and, therefore, Δy for (1,1) were recalculated until the mass efflux was within 1% of the mass influx for this element.

The final value of the shock-wave angle for element (1,1) was used as the initial guess for the shock-wave angle for the

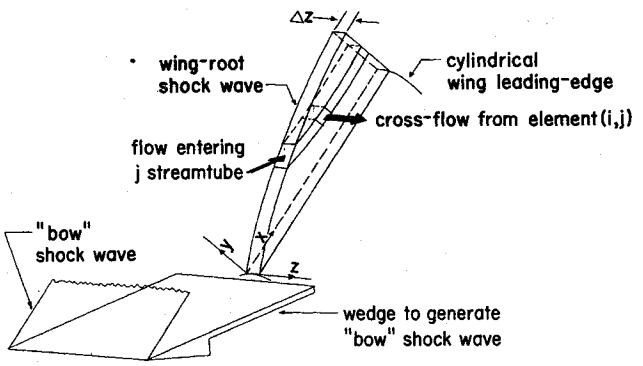

Fig. 2 Sketch of the theoretical model for the flowfield in the wing-root region.

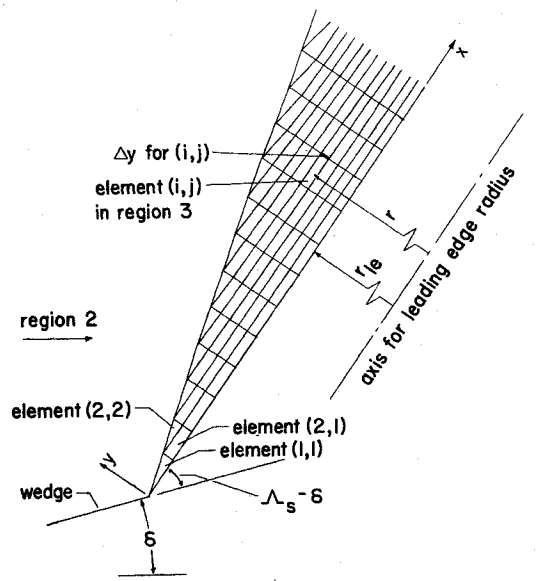

Fig. 3 The inviscid-flow streamline pattern for the plane of symmetry.

second streamwise station. Given the flow properties in region 2 and the shock-wave angle, the static pressure and flow direction for element (2,2) were calculated. For the initial iteration, the pressure was assumed to be constant across the shock layer, i.e., independent of y. The remaining properties for the internal element (2,1) were calculated assuming an isentropic acceleration from element (1,1), i.e., the entropy was constant along a streamline. The flow direction was specified as being parallel to the wall for each element $(i,1)$ adjacent to the surface except for element (1,1), where the flow direction was determined by the resultant shock-wave angle. The flow directions for intermediate elements were assumed to vary linearly from the shock, element (i,i), to the wall, element $(i,1)$. The direction of the flow in each element was used to construct the streamlines and to calculate the radius of curvature for each streamline. Once the radius of curvature for each streamline was known at the station, the pressure gradient normal to the surface was defined as

$$dp/dy = \rho u^2/r_s \tag{3}$$

Starting with the element immediately downstream of the shock wave, the pressure distribution across the shock layer was recalculated while accounting for the pressure variation caused by streamline curvature at the streamwise station. The remaining flow properties for each element were calculated assuming the entropy along a streamline to be constant. Using the "improved" flow properties, Δy (see Fig. 3) was calculated for each rectangular element by equating the efflux

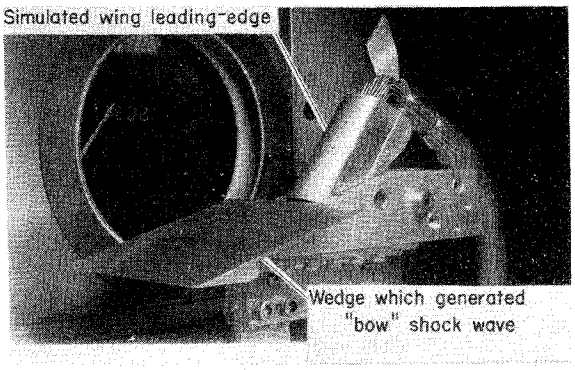

Fig. 4 Wedge:cylinder configuration used in the test program.

(including cross-flow) with the mass influx for that element. At this point, the mass influx for the triangular element (i,i) just downstream of the shock wave was compared to the efflux. The mass influx was calculated using the current value of the shock-wave angle. The value of Δy of element (i,i) needed to calculate the mass efflux from the element, including cross-flow, was calculated by subtracting the sum of the Δy's for the rectangular elements from the shock-layer thickness, which was calculated using the shock-wave angle and the shock-layer thickness at the previous station. If the mass efflux was not within 1% of the mass influx, the shock-wave angle was corrected, and the iterative procedure for calculating the pressure distribution across the shock layer was repeated. The calculation of the values of Δy for the rectangular elements and of the pressure distribution across the shock layer was repeated until successive values of the surface pressure agreed to within 0.1%.

The procedure was used at successive streamwise stations until the inviscid flowfield for region 3 has been defined. The properties of the inviscid flow at the surface served as the edge boundary-conditions for the boundary layer, which was assumed to originate at the root of the cylinder. The heat-transfer distribution for the plane-of-symmetry of the swept cylinder was calculated using a code for a nonsimilar, laminar boundary-layer.[10] The axisymmetric analog[11] was used to describe the three-dimensional character of the boundary layer. The metric-coefficient distribution, which describes the streamline divergence, was calculated using the relation[12]

$$dh = h(1/u)(dw/dz)dx \tag{4}$$

The radius of the cylindrical leading-edge was used as the value of the metric of the initial streamwise station, i.e., at the wing-root station.

Experimental Investigation

Test Conditions and Model

Because of the approximations inherent in the numerical code, an experimental program was conducted in the University of Texas Supersonic Wind Tunnel to insure that the theoretical flow model provided suitable engineering solutions. The freestream Mach number for the tests was 4.97 ± 0.02. The stagnation pressure was 2.01×10^6 N/m^2 (292 psia), with a maximum fluctuation during a run of $\pm 1.379 \times 10^4$ N/m^2 (± 2 psia). The stagnation temperature was 325 K (585°R). As a result the nominal freestream Reynolds number was 0.517×10^6/cm (15.7×10^6/ft).

A photograph of the wedge:cylinder configuration used during the test program is shown in Fig. 4. The wedge, which was 8.26 cm (3.25 in.) in length streamwise, by 7.42 cm (2.92 in.) in width, was inclined 15° to the freestream. A slab plate with a hemi-cylindrical leading edge represented the wing-leading edge. The radius of the cylinder was 0.945 cm (0.372 in.), the length 5.28 cm (2.08 in.). The sweep angle of the

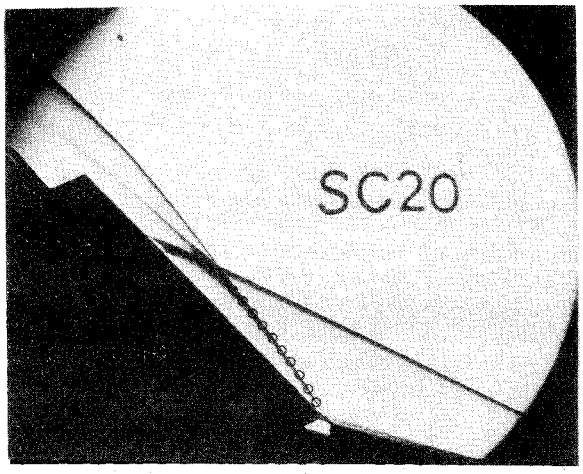

Fig. 5 Schlieren photograph of the Type VI shock-interaction pattern, $M_\infty = 4.97$, $\delta = 15°$, $\Lambda = 45°$. Theoretical location of wing-root shock wave is indicated by the symbol ○.

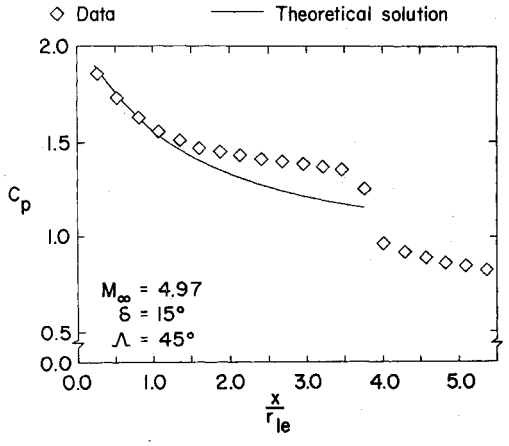

Fig. 6 Static-pressure distribution in plane of symmetry for cylindrical leading edge.

cylinder was varied from 30° to 70°. During the tests, a constant gap of 0.178 cm (0.070 in.) was maintained between the wedge and the upstream end of the cylinder to allow for boundary-layer bleed off and, thus, to minimize the possibility of separation in the corner interaction.

Flowfield

The theoretical solution for the wing-root shock wave is compared in Fig. 5 with the experimental shock wave for $\Lambda = 45°$. For this sweep angle, the shock-interaction pattern was Type VI. The agreement between the theoretical and the experimental shock wave in the wing-root region, i.e., region 3, was excellent. Furthermore, weak (Mach) waves which occurred when the flow at the surface of the swept cylinder was perturbed by the static-pressure orifices were evident in many of the schlieren photographs taken during the program. Experimental values for the local Mach number were calculated using the measured wave angles. The experimentally-determined values for the local Mach number were in good agreement with theory over the range of sweep angles tested.

Table 1 Flow conditions

Flow condition	U_∞ m/sec(fps)	M_∞	p_∞ mmHg(psia)	T_∞ K(°R)
FC1, a wind-tunnel condition	1167 (3829)	8.00	2.98 (0.57)	53 (95)
FC2, a hypothetical flight condition	1167 (3829)	3.42	760 (14.7)	288 (519)
FC3, an Orbiter entry condition	4330 (14,200)	13.08	0.333 (0.0064)	273 (491)
FC4, an Orbiter entry condition	7610 (25,000)	27.19	0.0268 (0.00052)	195 (352)
FC5, an Orbiter entry condition	4330 (14,200)	15.45	0.0268 (0.00052)	195 (352)

The static pressure measurements from the plane-of-symmetry of the swept cylinder are presented in Fig. 6. Also included is the theoretical distribution, as calculated using the numerical code described previously. For the orifice nearest the root, the experimental pressure was within 1.4% of the theoretical value. For the orifice at the downstream end of region 3, the experimental pressure was 18% higher than the theoretical value. The pressures are consistent with Fig. 5, since the measured shock-layer thickness was slightly greater than the theoretical value at the downstream end of region 3. The effect of the boundary-layer displacement thickness would contribute to the difference between experiment and theory. Reference 13 gives additional information about the test program.

The correlation with the theoretical solutions indicated in the data of Figs. 5 and 6 are typical of the results obtained in the present experimental program. Thus, the theoretical flow model does provide a suitable engineering solution.

Theoretical Heat-Transfer Correlations

Numerical solutions for nonsimilar, laminar boundary layers[10] were generated to determine the effect of the freestream conditions and of the wall temperature on the heat transfer for the three-dimensional flow in region 3. Perfect-air flowfield solutions were generated for the five freestream conditions of Table 1. Flow condition 3 corresponds to an altitude of approximately 54.5 km (179,000 ft), while flow condition 4 and 5 correspond to an altitude of approximately 73.2 km (240,000 ft).

The heat-transfer calculations for the plane of symmetry are presented in Figs. 7-9 as the ratio of the local heat-transfer coefficient h to the reference, stagnation-point heat-transfer coefficient $h_{t,\mathrm{ref}}$. The recovery temperature $T_r = 0.837 (T_t - T_e) + T_e$ was calculated using the inviscid-flow solutions, but was approximately constant in region 3 for the solutions of Figs. 7-9. The stagnation-point heating rate[14] is that for a reference sphere whose radius is 0.305 m (1.0 ft) and which is at the same temperature and subjected to the same freestream flow as the cylindrical surface.

The heat-transfer distributions from the plane of symmetry are presented in Fig. 7 for the five flow conditions. The cylindrical leading-edge was swept 80°. The surface temperature for these calculations was 300K (540°R). Note that the dimensionless ratio of the heat-transfer coefficients is not independent of the flow conditions. In fact, the nondimensionalized heat-transfer coefficients were greatest for flow condition 2 and the least for flow condition 1, even though the freestream velocity was the same for these two conditions and was relatively low. The nondimensionalized heat-transfer coefficients were essentially the same for conditions 3 and 5, for which the velocity was the same, and relatively high, but the altitude different. For conditions 4 and 5, which represent the same altitude, the nondimensionalized heat transfer increased with freestream velocity. Thus, one should not use the ratio of $h/h_{t,\mathrm{ref}}$, or $\dot{q}/\dot{q}_{t,\mathrm{ref}}$, to extrapolate wind-tunnel data directly to flight conditions.

Condition 1 was selected from one of the Shuttle wind-tunnel programs. As is typical of hypersonic wind-tunnels, the freestream static-temperature was as low as possible so that the Mach number would be hypersonic without subjecting the facility hardware to excessively high temperatures. Thus, although the freestream velocity was the same for conditions 1 and 2, the stagnation temperature and the freestream Mach number and, therefore, the local Mach number along the cylindrical leading-edge, were markedly different. Con-

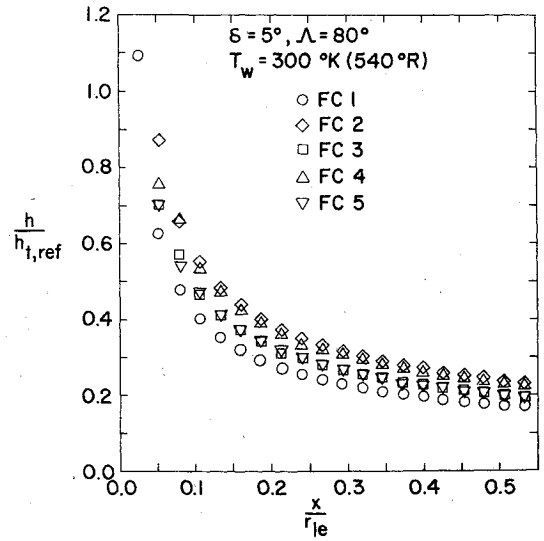

Fig. 7 The effect of freestream conditions on the theoretical heat-transfer distribution in the plane of symmetry.

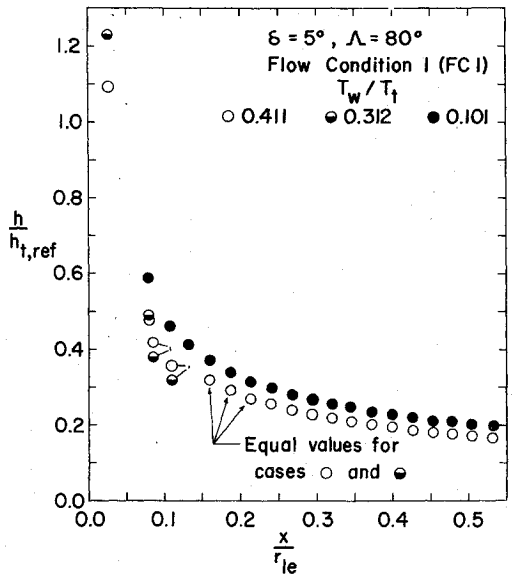

Fig. 8 The effect of surface temperature on the theoretical heat-transfer distribution in the plane of symmetry.

sidering the resulting differences between the temperature ratios, for conditions 1 and 2, the heat-transfer differences of Fig. 7 were not surprising. The effect of surface temperature on the heat-transfer distribution for flow condition 1 is presented in Fig. 8. Theoretical solution are presented for the following wall temperatures: 1) 300K (540°R), i.e., the assumed standard value for the theoretical solutions, which was 0.411 T_t; 2) 277K (409°R), for which T_w was 0.312 T_t, the same value as condition 2; and 3) 74K (133°R), which corresponds to the nominal value of the static temperature at the edge of the boundary layer. The nondimensionalized heat-transfer coefficients were greatest for the case with the lowest wall temperature. However, despite the considerable variations in the wall temperature, the dimensionless heat transfer for flow condition 1 remained less than that for flow condition 2 (see Fig. 9a).

As has been discussed, division of the local heat-transfer coefficients by $h_{t,ref}$ yielded a dimensionless parameter which is not independent of the flow conditions. The nondimensionalized heat-transfer coefficients at a point 0.305 m (1.0 ft.), i.e., $x = 0.533\ r_{le}$, from the root of the cylinder are presented as a function of the freestream velocity in Fig. 9 for

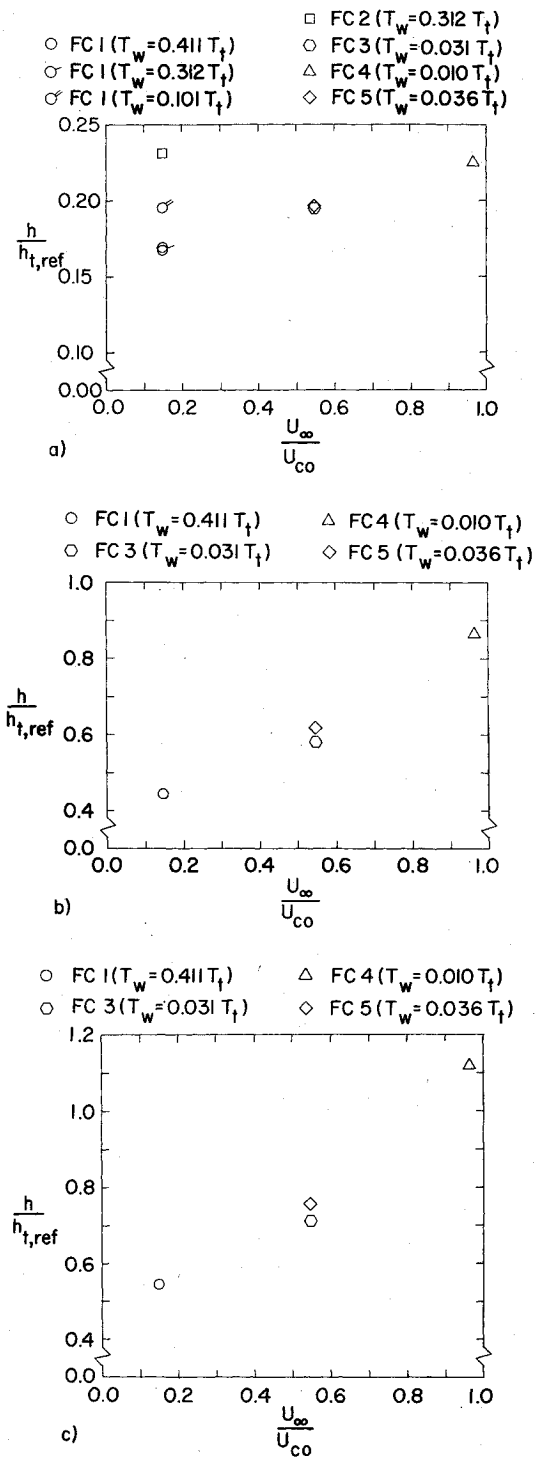

Fig. 9 The effect of freestream velocity on the heating at $x = 0.533\ r_{le}$ in region 3: a) $\Lambda = 80°$; b) $\Lambda = 60°$; c) $\Lambda = 50°$.

Λ of 80°, 60°, and 50°. The dimensionless heating for the higher entry velocity was approximately twice the value for the wind tunnel condition (with the surface temperature the same for both flows). Thus, the "velocity-dependent" increase for the "three-dimensional" flow of the present investigation was approximately equal to the increase for the two-dimensional flows of Ref. 8. However, the difference between the theoretical values for the three solutions for flow condition 1 and the relatively high values for flow condition 2 indicate the need to include additional parameters in the correlations.

A correlation, which can be used for a wide variety of conditions, was obtained using local properties to non-

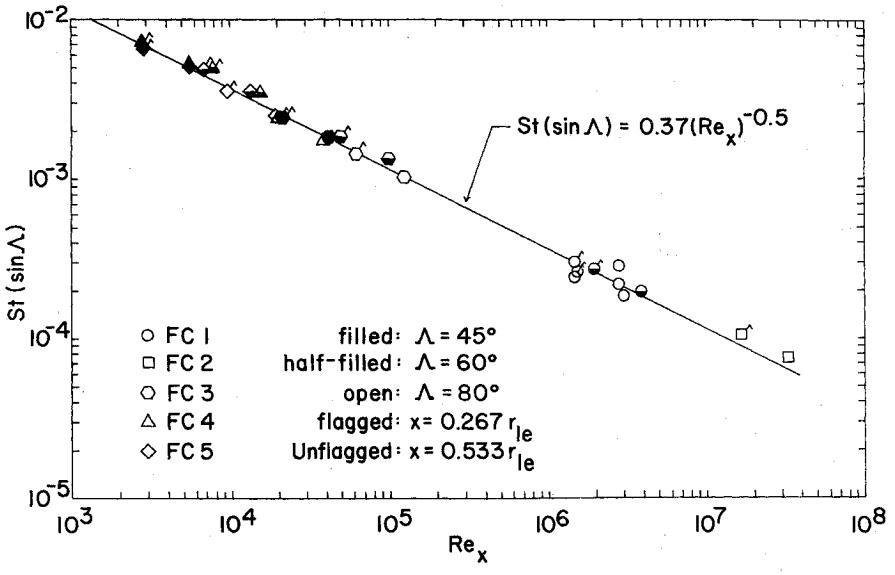

Fig. 10 Heat transfer correlation in terms of local flow conditions.

dimensionalize the heat-transfer as shown in Fig. 10. The theoretical local Stanton number was calculated as

$$St = \dot{q}/\rho_e u_e (h_r - h_w) \tag{5}$$

where the subscript e denotes that the properties are evaluated at the edge of the boundary layer. The local Reynolds number was calculated as

$$Re_x = \int \frac{\rho_e u_e}{\mu_e} dx \tag{6}$$

A least-squares fit of the theoretically determined Stanton numbers presented in Fig. 10 produced the relation

$$St\ (\sin \Lambda) = 0.37\ (Re_x)^{-0.5} \tag{7}$$

The correlation applies to all five freestream conditions, for the three wall temperatures considered for flow condition 1, and for sweep angles from 45° to 80°. Since perfect gas relations were used and δ was 5°, numerical solutions for the flow model of interest could not be obtained for sweep angles significantly out of this range.

Thus, the wind-tunnel data should be used to construct a viable model of the flowfield. The flowfield model can be used to generate the trends in the aerothermodynamic environment at the conditions of interest. Through proper calibration of this model (using wind tunnel data from the corresponding double-shock region of the Orbiter), an engineering tool can be constructed for predicting both the trends and magnitudes of the wing edge heating rates during entry. (Note that this model was not designed to simulate the very localized shock-interaction-induced boundary-layer perturbation on the wing leading-edge.

Concluding Remarks

An easily coded streamtube model has been developed for simulating the flowfield in the plane of symmetry for the "Shuttle wing-leading-edge" inboard of the shock interaction. Correlations between the theoretical solutions and the pressure and shock-shape data obtained in an experimental program have been used to calculate the heat transfer to the cylindrical leading-edge for perfect-gas flows at conditions typically used in wind-tunnel testing as well as entry conditions. Based on the calculations of the present study, the following conclusions are made.

1) Division of the local heat-transfer coefficient by a reference coefficient yielded a dimensionless parameter, the value of which depended on the freestream conditions and on the surface temperature, and which, when used alone, cannot be used to accurately predict entry heating rates. The nondimensionalized heat-transfer coefficient for the higher entry velocity was approximately twice the value for the wind-tunnel condition.

2) Nondimensionalization of the heat-transfer rates in terms of local flow parameters produced a correlation of Stanton number as a function of Reynolds number based on length, which was independent of the flow conditions and of the surface temperature.

3) Relative to heating-rate predictions at wind tunnel conditions, both "three-dimensional" and two-dimensional flow models predict similar changes in heating when extrapolated to the flight conditions.

References

[1]Hiers, R. S. and Loubsky, W. J., "Effects on Shock-Wave Impingement on the Heat Transfer on a Cylindrical Leading Edge," NASA TND-3859, Feb. 1967.

[2]Beckwith, I. E., "Experimental Investigation of Heat Transfer and Pressures on a Swept Cylinder in the Vicinity of Its Intersection with a Wedge and Flate Plate at Mach Number 4.15 and High Reynolds Numbers," NASA TND-2020, July 1964.

[3]Bushnell, D. M., "Interference Heating on a Swept Cylinder in Region of Intersection with a Wedge at Mach Number of 8," NASA TND-3094, Dec. 1965.

[4]Edney, B., "Anomalous Heat Transfer and Pressure Distributions on Blunt Bodies at Hypersonic Speeds in the Presence of an Impinging Shock," Flygteckniska Forsoksanstalten (The Aeronautical Research Institute of Sweden), Stockholm, Rept. 115, 1968.

[5]Hains, F. D. and Keyes, J. W., "Shock Interference Heating in Hypersonic Flows," *AIAA Journal*, Vol. 10, Nov. 1972, pp. 1441-1447.

[6]Bertin, J. J., Graumann, B. W., and Goodrich, W. D., "Aerothermodynamic Aspects of Shock-Interference Patterns for Shuttle Configurations During Entry," *Journal of Spacecraft and Rockets*, Vol. 10, Sept. 1973, pp. 545-546.

[7]Hunt, J. L. and Creel, T. R. Jr., "Shock-Interference Heating and Density-Ratio Effects, Pt. II: Hypersonic Density-Ratio Effect," NASA Space Shuttle Technology Conference, Vol. I; Aerothermodynamics, Configurations and Flight Mechanics, NASA TMX-2272, April 1971.

[8]Bertin, J. J., Graumann, B. W., and Goodrich, W. D., "High Velocity and Real-Gas Effects on Weak Two-Dimensional Shock-Interaction Patterns," *Journal of Spacecraft and Rockets*, Vol. 12, March 1975, pp. 155-161.

[9]Bertin, J. J. and Hinkle, J. C., "Experimental Investigation of Supersonic Flow Past Double-Wedge Configurations," *AIAA Journal*, Vol. 13, July 1975, pp. 897-901.

[10]Bertin, J. J. and Byrd, O. E., Jr., "The Analysis of a Nonsimilar Boundary Layer-A Computer Code (NON SIMBL)," University of Texas, Austin, Texas, Aerospace Engineering Rept. 70002, Aug. 1970.

[11]Cooke, J. C., "An Axially Symmetric Analogue for General Three-Dimensional Boundary Layers," British Aeronautical Research Council, R&M 3200, 1961.

[12]Rakich, J. V. and Mateer, G. G., "Calculation of Metric Coefficients for Streamline Coordinates," *AIAA Journal*, Vol. 10, Nov. 1972, pp. 1538-1540.

[13]Barnette, D. W., "An Experimental Investigation of Supersonic Flow Past a Wedge:Cylinder," University of Texas, Austin, Texas, Aerospace Engineering Rept. 76002, April 1976.

[14]Fay, J. A. and Riddell, F. R., "Theory of Stagnation Point Heat Transfer in Dissociated Air," *Journal of Aeronautical Sciences*, Vol. 10, Feb. 1958, pp. 73-85, 121.